REFLECTION PROPERTIES OF A BIAXIALLY ANISOTROPIC DIELECTRIC FILM IN A LONG-WAVELENGTH APPROXIMATION

P. Adamson

Institute of Physics
University of Tartu, Riia 142, Tartu 51014, Estonia

Abstract—The reflection of linearly polarized light from an ultrathin biaxially anisotropic dielectric film on an isotropic transparent material is investigated in the long-wavelength limit. The approximate expressions for the reflection characteristics of s- and p-polarized electromagnetic plane waves are obtained. The analytical approach developed in this paper not only provides insight into the nature of reflection problem for biaxially anisotropic ultrathin films but also furnishes the methods for resolving the inverse problem for such anisotropic layers. It is shown that a key capability of the developed analytical method is to decouple the usual correlations in the index and the thickness of ultrathin films.

1. INTRODUCTION

Anisotropic dielectric films play an important role already for a long time in a number of modern optical systems such a guided-wave propagation in integrated optics or narrow-band polarization filters in conventional optics [1, 2]. In addition, at present, dielectric layers have also grown in importance in the technology of micro- and nanoelectronic devices [3, 4]. Notably advances in nanotechnology have raised the issue of novel diagnostics techniques with greater capabilities for the analysis of ultrathin anisotropic layered structures.

Well-accepted methods for optical characterization of an ultrathin film (thickness d is much less than an optical wavelength λ) are differential reflection techniques [5–8], which are founded on direct measurement of the contribution of an ultrathin layer to the reflection coefficient or ellipsometric angles. The heart of

the theory of differential reflection methods is a long-wavelength approximation [9]. This approximation is of critical importance particularly for anisotropic thin-film systems because it enables one to derive the relatively simple analytical relationships for reflection characteristics. These analytical expressions not only give a physical insight into the details of the reflection process, but also are especially advantageous for tackling the inverse problem. The reason is that the creation a solution for the inversion problem for an anisotropic layered system is rather intricate process owing to the complexity of the corresponding exact reflection equations. In general, these equations cannot analytically be inverted, and the solution of such problems can only be found by the use of complicated numerical methods. But these methods, as a rule, come across serious difficulties, the main two being the instability and the nonuniqueness of the solution. In addition, it is important to note that the analytical algorithms for calculating the parameters of interest directly from the measured data are very fast in comparison with classical, e.g., the regressive type of algorithms. Because of this fact, approximate analytical techniques are also used to provide initial guesses at the values of the variable parameters, and regression techniques are then used to fine tune the desired parameters.

Until the present time only few investigations have been done to find out how the differential reflection methods can be used for determining the parameters of anisotropic ultrathin dielectric films on absorbing [10–12] or transparent substrates [13, 14]. In [13], general long-wave limit formulas for reflection characteristics of an N-layer system of anisotropic dielectric films on isotropic dielectric substrates are derived. In [14], the possibilities for reflection characterization of biaxially anisotropic ultrathin films are discussed only in the case where the thickness of such layers is a predetermined quantity.

A purpose of this paper is to study the reflection properties of biaxially anisotropic nonmagnetic dielectric films on transparent isotropic bulk in the long-wavelength approximation and to work out the differential reflection method for optical diagnostics of biaxially anisotropic ultrathin films in the general case where the film thickness is also an unknown quantity.

The paper is organized as follows. In Section 2, the second-order expression in the long-wave limit for 4×4 transfer matrix of an anisotropic layer on a transparent isotropic substrate is produced. In Sections 3, the final analytical expressions for the reflection and transmission coefficients are derived. In Section 4, the approximate analytical results are correlated with the exact numerical solution of the reflection problem for anisotropic systems. The fifth section is concerned with the solution of the inverse problem on the basis of

obtained formulas for reflection characteristics. It must be emphasized that a key capability of such analytical expressions is to decouple the usual correlations in the index and the thickness of ultrathin films.

2. 4×4 TRANSFER MATRIX

Assuming that all the media are nonmagnetic, we consider the reflection of s- and p-polarized time-harmonic (the complex representation is taken in the form $\exp(-i\omega t)$, where $\omega = 2\pi c/\lambda$, and λ is a vacuum wavelength) electromagnetic plane waves in an ambient medium with isotropic and homogeneous dielectric constant $\varepsilon_a \equiv n_a^2$ from an anisotropic homogeneous dielectric film of thickness $d \ll \lambda$ and with principal dielectric-tensor components in the crystal-coordinate system $\varepsilon_{xx} = n_{xx}^2$, $\varepsilon_{yy} = n_{yy}^2$, and $\varepsilon_{zz} = n_{zz}^2$ that is located upon a semi-infinite isotropic and homogeneous substrate with dielectric constant $\varepsilon_s \equiv n_s^2$ (Fig. 1). The orientations of the crystal axes are described by the Euler angles θ, φ, and ψ with respect to a fixed xyz coordinate system (the Cartesian laboratory coordinate system). The laboratory x, y, and z axes are defined as follows. The reflecting surface is the xy plane, and the plane of incidence is the zx plane, with the z axis normal to the surface of the layered medium and directed into it. The incident light beam in the ambient medium makes an angle ϕ_a with the z axis.

The dielectric tensor for an anisotropic layer in the xyz coordinate
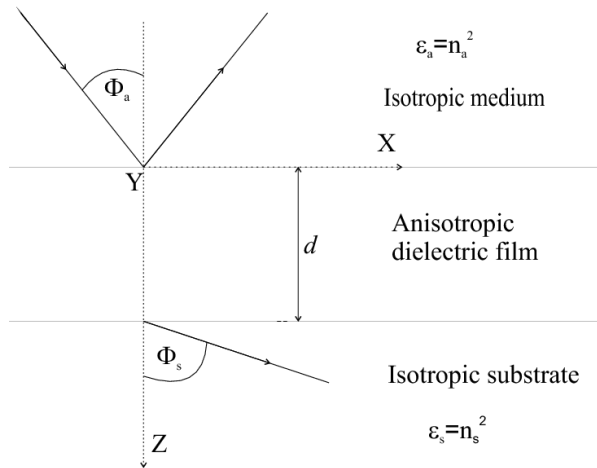
Figure 1. Schematic cross section of the simulation structure.

system is given by

$$
\begin{bmatrix} \varepsilon_{11} & \varepsilon_{12} & \varepsilon_{13} \\ \varepsilon_{21} & \varepsilon_{22} & \varepsilon_{23} \\ \varepsilon_{31} & \varepsilon_{32} & \varepsilon_{33} \end{bmatrix} = \mathbf{A} \begin{bmatrix} \varepsilon_{xx} & 0 & 0 \\ 0 & \varepsilon_{yy} & 0 \\ 0 & 0 & \varepsilon_{zz} \end{bmatrix} \mathbf{A}^{-1}, \tag{1}
$$

where $\mathbf{A}$ is the coordinate rotation matrix [15]. Therefore,

$$
\begin{aligned}
\varepsilon_{11} &= -\Gamma_1 \sin 2\varphi \sin 2\psi \cos \theta + \Gamma_2 \cos^2 \varphi \\
&\quad + \Gamma_3 \sin^2 \varphi \cos^2 \theta + \varepsilon_{zz} \sin^2 \varphi \sin^2 \theta, \tag{2}
\end{aligned}
$$

$$
\begin{aligned}
\varepsilon_{22} &= \Gamma_1 \sin 2\varphi \sin 2\psi \cos \theta + \Gamma_2 \sin^2 \varphi \\
&\quad + \cos^2 \varphi \left(\Gamma_3 \cos^2 \theta + \varepsilon_{zz} \sin^2 \theta \right), \tag{3}
\end{aligned}
$$

$$
\varepsilon_{33} = \Gamma_3 \sin^2 \theta + \varepsilon_{zz} \cos^2 \theta, \tag{4}
$$

$$
\begin{aligned}
\varepsilon_{12} &= \varepsilon_{21} = \Gamma_1 \cos 2\varphi \sin 2\psi \cos \theta \\
&\quad + \sin 2\varphi \left(\Gamma_2 - \Gamma_3 \cos^2 \theta - \varepsilon_{zz} \sin^2 \theta \right) / 2, \tag{5}
\end{aligned}
$$

$$
\varepsilon_{13} = \varepsilon_{31} = \sin \theta \left[\Gamma_1 \cos \varphi \sin 2\psi - \sin \varphi \cos \theta \left(\Gamma_3 - \varepsilon_{zz} \right) \right], \tag{6}
$$

$$
\varepsilon_{23} = \varepsilon_{32} = \sin \theta \left[\Gamma_1 \sin \varphi \sin 2\psi + \cos \varphi \cos \theta \left(\Gamma_3 - \varepsilon_{zz} \right) \right], \tag{7}
$$

where

$$
\begin{aligned}
&\Gamma_1 \equiv (\varepsilon_{xx} - \varepsilon_{yy})/2, \quad \Gamma_2 \equiv \varepsilon_{xx} \cos^2 \psi + \varepsilon_{yy} \sin^2 \psi, \\
&\Gamma_3 \equiv \varepsilon_{xx} \sin^2 \psi + \varepsilon_{yy} \cos^2 \psi. \tag{8}
\end{aligned}
$$

In a similar manner to the isotropic case, we use the matrix method for calculating the contributions of anisotropic layers to the reflection characteristics. Since s and p modes are no longer spatially independent of each other (a so-called mode coupling appears) in the anisotropic medium, then, consequently, 4×4 matrices are needed in order to establish an analogous matrix method. Dealing directly with first-order Maxwell equations, we can calculate the reflection characteristics of an anisotropic layered system from a wave transfer matrix of rank 4 [16] (note that the other way is to work with corresponding second-order wave equations [1]). The 4×4-matrix method consists of calculating a 4×4 characteristic matrix, $\mathbf{B}(d)$, such that

$$
\begin{bmatrix} E_x \\ H_y \\ E_y \\ -H_x \end{bmatrix}_{z=d} = \mathbf{B}(d) \begin{bmatrix} E_x \\ H_y \\ E_y \\ -H_x \end{bmatrix}_{z=0} \tag{9}
$$

or

$$
\Xi(d) = \mathbf{B}(d)\Xi(0), \tag{10}
$$

where $E_{x,y}$ and $H_{x,y}$ are the electric and magnetic field components parallel to the interfaces.

On the other hand, on the basis of Maxwell's equations

$$\text{curl}\vec{E} = i(\omega/c)\vec{H},$$
$$\text{curl}\vec{H} = -i(\omega/c)\vec{D}, \tag{11}$$

or

$$\frac{\partial E_y}{\partial z} = -i(\omega/c)H_x,$$
$$ik_x E_z - \frac{\partial E_x}{\partial z} = -i(\omega/c)H_y,$$
$$k_x E_y = (\omega/c)H_z,$$
$$\frac{\partial H_y}{\partial z} = i(\omega/c)D_x,$$
$$-ik_x H_z + \frac{\partial H_x}{\partial z} = -i(\omega/c)D_y,$$
$$k_x H_y = -(\omega/c)D_z,$$

and of constitutive relations

$$D_x = \varepsilon_{11}E_x + \varepsilon_{12}E_y + \varepsilon_{13}E_z,$$
$$D_y = \varepsilon_{21}E_x + \varepsilon_{22}E_y + \varepsilon_{23}E_z, \tag{12}$$
$$D_z = \varepsilon_{31}E_x + \varepsilon_{32}E_y + \varepsilon_{33}E_z,$$

we obtain the following system of equations:

$$\frac{\partial E_x}{\partial z} = i[(\omega/c)H_y + k_x E_z], \tag{13}$$

$$\frac{\partial H_y}{\partial z} = i(\omega/c)[\varepsilon_{11}E_x + \varepsilon_{12}E_y + \varepsilon_{13}E_z], \tag{14}$$

$$\frac{\partial E_y}{\partial z} = -i(\omega/c)H_x, \tag{15}$$

$$\frac{\partial H_x}{\partial z} = -i(\omega/c)[\varepsilon_{21}E_x + \varepsilon_{22}E_y + \varepsilon_{23}E_z] + ik_x H_z, \tag{16}$$

$$H_z = k_x(c/\omega)E_y, \tag{17}$$

$$E_z = -\varepsilon_{33}^{-1}[k_x(c/\omega)H_y + \varepsilon_{31}E_x + \varepsilon_{32}E_y], \tag{18}$$

where $\vec{D}$ is the electric displacement and $k_x = (\omega/c)n_a \sin\phi_a$. Note that the component of the propagation vector in the x direction k_x is a constant and there is no y component. Solutions in this case have the common factor $\exp(ik_x x)$.

Therefore, a differential form of the Equation (10) may be written {by substituting Equations (17) and (18) into (13)–(16)}

$$\frac{\partial}{\partial z}\Xi(z) = \frac{i2\pi}{\lambda}\mathbf{C}\Xi(z), \tag{19}$$

$$\mathbf{C} = \begin{bmatrix} c_{11} & c_{12} & c_{13} & 0 \\ c_{21} & c_{11} & c_{23} & 0 \\ 0 & 0 & 0 & 1 \\ c_{23} & c_{13} & c_{43} & 0 \end{bmatrix}, \tag{20}$$

where $c_{11} = -n_a \sin \phi_a \varepsilon_{13}/\varepsilon_{33}$, $c_{12} = 1 - \varepsilon_a \sin^2 \phi_a/\varepsilon_{33}$, $c_{13} = -n_a \sin \phi_a \varepsilon_{23}/\varepsilon_{33}$, $c_{21} = \varepsilon_{11} - \varepsilon_{13}^2/\varepsilon_{33}$, $c_{23} = \varepsilon_{12} - \varepsilon_{13}\varepsilon_{23}/\varepsilon_{33}$, $c_{43} = \varepsilon_{22} - \varepsilon_{23}^2/\varepsilon_{33} - \varepsilon_a \sin^2 \phi_a$.

A fitting procedure for finding $\mathbf{B}(d)$ in the long-wavelength approximation is simply to integrate Eq. (19). Because the matrix $\mathbf{C}$ is independent of z over the finite distance d in the direction of the z axis, it is evident that the solution is

$$\Xi(z) = \exp(i2\pi \, \mathbf{C} \, z/\lambda). \tag{21}$$

Thus,

$$\Xi(z + d) = \mathbf{B}(d)\Xi(z) = \exp[i2\pi \, \mathbf{C} \, d/\lambda]\Xi(z), \tag{22}$$

and

$$\mathbf{B}(d) = \exp[i2\pi \, \mathbf{C} \, d/\lambda]. \tag{23}$$

Within the framework of the long-wavelength limit ($d \ll \lambda$), we can use the Taylor-series-like expansion, which in the first order with respect to the small parameter d/λ yields:

$$\mathbf{B}_{ap}(d) = \left[\mathbf{I} + i2\pi\mathbf{C} \, d/\lambda - 2\pi^2[\mathbf{C}]^2 d^2/\lambda^2 \right], \tag{24}$$

where $\mathbf{B}_{ap}(d)$ is the approximate transfer matrix and $\mathbf{I}$ is the 4×4 identity (unit) matrix.

Hence, the second-order expression for the 4×4 approximate transfer matrix $\mathbf{B}_{ap}$ takes the form:

$$\mathbf{B}_{ap}(d) = \begin{bmatrix} b_{11} & b_{12} & b_{13} & b_{14} \\ b_{21} & b_{11} & b_{23} & b_{24} \\ b_{24} & b_{14} & b_{33} & b_{34} \\ b_{23} & b_{13} & b_{43} & b_{33} \end{bmatrix}, \tag{25}$$

in which

$$b_{11} = 1 + i2\pi c_{11}(d/\lambda) - 2\pi^2 \left([c_{11}]^2 + c_{12}c_{21}\right)(d/\lambda)^2,$$
$$b_{12} = i2\pi c_{12}(d/\lambda) - 4\pi^2 c_{11}c_{12}(d/\lambda)^2,$$
$$b_{13} = i2\pi c_{13}(d/\lambda) - 2\pi^2(c_{11}c_{13} + c_{12}c_{23})(d/\lambda)^2,$$
$$b_{14} = -2\pi^2 c_{13}(d/\lambda)^2$$
$$b_{21} = i2\pi c_{21}(d/\lambda) - 4\pi^2 c_{11}c_{21}(d/\lambda)^2,$$
$$b_{23} = i2\pi c_{23}(d/\lambda) - 2\pi^2(c_{21}c_{13} + c_{11}c_{23})(d/\lambda)^2,$$
$$b_{24} = -2\pi^2 c_{23}(d/\lambda)^2$$
$$b_{33} = 1 - 2\pi^2 c_{43}(d/\lambda)^2$$

$$b_{34} = i2\pi(d/\lambda),$$
$$b_{43} = i2\pi c_{43}(d/\lambda) - 4\pi^2 c_{13}c_{23}(d/\lambda)^2.$$

Note that, $[\mathbf{B}(d)]^{-1} = \mathbf{B}(-d)$.

3. REFLECTION AND TRANSMISSION COEFFICIENTS

The electromagnetic field in the ambient medium is made up of two parts, the incident- and the reflected-wave contributions, $\Xi^{(a)} = \Xi_I^{(a)} + \Xi_R^{(a)}$, and the field in the isotropic substrate matches solely a transmitted wave field, $\Xi^{(s)}$. Since in the media (a) and (s) field components are $H_{Iy}^{(a)} = (n_a/\cos\phi_a)E_{Ix}^{(a)}$, $-H_{Ix}^{(a)} = n_a\cos\phi_a E_{Iy}^{(a)}$, $H_{Ry}^{(a)} = -(n_a/\cos\phi_a)E_{Rx}^{(a)}$, $H_{Rx}^{(a)} = n_a\cos\phi_a E_{Ry}^{(a)}$, $H_y^{(s)} = (n_s/\cos\phi_s)E_x^{(s)}$, and $-H_x^{(s)} = n_s\cos\phi_s E_y^{(s)}$, where $\cos\phi_s = (1 - \varepsilon_a\varepsilon_s^{-1}\sin^2\phi_a)^{1/2}$, then from the matrix equation

$$\Xi_I^{(a)} + \Xi_R^{(a)} = \mathbf{B}_{ap}^{-1}\Xi^{(s)}, \qquad (26)$$

one can obtain four linear equations:

$$E_{Ix}^{(a)} + E_{Rx}^{(a)} = b_{11}E_x^{(s)} + \frac{n_s}{\cos\phi_s}b_{12}E_x^{(s)} + b_{13}E_y^{(s)},$$

$$\frac{n_a}{\cos\phi_a}\left(E_{Ix}^{(a)} - E_{Rx}^{(a)}\right) = b_{21}E_x^{(s)} + \frac{n_s}{\cos\phi_s}b_{11}E_x^{(s)} + b_{23}E_y^{(s)},$$

$$E_{Iy}^{(a)} + E_{Ry}^{(a)} = E_y^{(s)} + n_s\cos\phi_s b_{34}E_y^{(s)},$$

$$n_a\cos\phi_a\left(E_{Iy}^{(a)} - E_{Ry}^{(a)}\right) = b_{23}E_x^{(s)} + \frac{n_s}{\cos\phi_s}b_{13}E_x^{(s)} + b_{43}E_y^{(s)} + n_s\cos\phi_s E_y^{(s)}.$$

We solve this system of equations for the two cases, first, if $E_{Iy}^{(a)} \equiv 0$ (p-polarized incident wave) and, second, if $E_{Ix}^{(a)} \equiv 0$ (s-polarized incident wave). In the case of p-polarization, we obtain for $r_{pp} = E_{Rx}^{(a)}/E_{Ix}^{(a)}$ (reflection coefficient) and $t_{pp} = [E_x^{(s)}/E_{Ix}^{(a)}]\cos\phi_a/\cos\phi_s$ (transmission coefficient) the following results:

$r_{pp} \approx$

$r_p^{(0)}\Big\{1 + i4\pi n_a\cos\phi_a\big(\varepsilon_a\cos^2\phi_s - \varepsilon_s\cos^2\phi_a\big)^{-1}\big(c_{21}\cos^2\phi_s - c_{12}\varepsilon_s\big)(d/\lambda)$

$+\big[(c_{12}\varepsilon_s - c_{21}\cos^2\phi_s)(c_{12}n_a n_s + c_{21}\cos\phi_a\cos\phi_s)(n_a\cos\phi_s + n_s\cos\phi_a)^{-1}$

$+\big(c_{13}^2\varepsilon_s - c_{23}^2\cos^2\phi_s\big)(n_a\cos\phi_a + n_s\cos\phi_s)^{-1}\big](d/\lambda)^2\Big\}, \qquad (27)$

$$t_{pp} = t_p^{(0)}\Big\{1 + i2\pi\left[c_{11} + \alpha\right](d/\lambda) + 2\pi^2(n_a\cos\phi_s - n_s\cos\phi_a)$$

$$-4\pi^2[(c_{13}n_s + c_{23}\cos\phi_s)(c_{13}n_a + c_{23}\cos\phi_a)(n_a\cos\phi_a + n_s\cos\phi_s)^{-1}$$

$$\times(n_a\cos\phi_s + n_s\cos\phi_a)^{-1} + (c_{11}^2 - c_{12}c_{21})/2 + \alpha\,(c_{11} + \alpha)\Big](d/\lambda)^2\Big\}, \quad (28)$$

$$\alpha \equiv (c_{12}n_a n_s + c_{21}\cos\phi_a\cos\phi_s)(n_a\cos\phi_s + n_s\cos\phi_a)^{-1},$$

where $r_p^{(0)}$ and $t_p^{(0)}$ are the amplitude reflection and transmission coefficient, respectively, from bare ($d \equiv 0$) isotropic substrate and are expressed by the standard Fresnel's formulas as

$$r_p^{(0)} = (n_a\cos\phi_s - n_s\cos\phi_a)/(n_a\cos\phi_s + n_s\cos\phi_a), \qquad (29)$$

$$t_p^{(0)} = 2n_a\cos\phi_a/(n_a\cos\phi_s + n_s\cos\phi_a). \qquad (30)$$

Analogously, in the case of s-polarized incident wave ($E_{Ix}^{(a)} \equiv 0$) for $r_{ss} = E_{Ry}^{(a)}/E_{Iy}^{(a)}$ and $t_{ss} = E_y^{(s)}/E_{Iy}^{(a)}$, we obtain:

$$r_{ss} = r_s^{(0)}\Big\{1 + i4\pi n_a\cos\phi_a\,(\varepsilon_a - \varepsilon_s)^{-1}\left(c_{43} - \varepsilon_s\cos^2\phi_s\right)(d/\lambda)$$

$$+\Big[\left(\varepsilon_s\cos^2\phi_s - c_{43}\right)(c_{43} + n_a n_s\cos\phi_a\cos\phi_s)(n_a\cos\phi_a + n_s\cos\phi_s)^{-1}$$

$$-\left(c_{13}^2 n_a n_s + c_{23}^2\cos\phi_a\cos\phi_s\right)(n_a\cos\phi_s + n_s\cos\phi_a)^{-1}\Big](d/\lambda)^2\Big\}, \quad (31)$$

$$t_{ss} = t_s^{(0)}\Big\{1 + i2\pi\beta(d/\lambda) - 4\pi^2\Big[\beta^2 + (c_{13}n_a + c_{23}\cos\phi_a)$$

$$\times(c_{13}n_s + c_{23}\cos\phi_s)(n_a\cos\phi_a + n_s\cos\phi_s)^{-1}(n_a\cos\phi_s + n_s\cos\phi_a)^{-1}$$

$$-c_{13}c_{23}(n_a\cos\phi_a + n_s\cos\phi_s)^{-1} - c_{43}/2\Big](d/\lambda)^2\Big\}, \qquad (32)$$

$$\beta \equiv (c_{43} + n_a n_s\cos\phi_a\cos\phi_s)(n_a\cos\phi_a + n_s\cos\phi_s)^{-1},$$

$$r_s^{(0)} = (n_a\cos\phi_a - n_s\cos\phi_s)/(n_a\cos\phi_a + n_s\cos\phi_s), \qquad (33)$$

$$t_s^{(0)} = 2n_a\cos\phi_a/(n_a\cos\phi_a + n_s\cos\phi_s). \qquad (34)$$

For the remaining quantities $r_{ps} = [E_{Ry}^{(a)}/E_{Ix}^{(a)}]\cos\phi_a$, $t_{ps} = [E_y^{(s)}/E_{Ix}^{(a)}]\cos\phi_a$, $r_{sp} = [E_{Rx}^{(a)}/E_{Iy}^{(a)}]/\cos\phi_a$, and $t_{sp} = [E_x^{(s)}/E_{Iy}^{(a)}]/\cos\phi_s$ (in this paper, the first subscript indicates the incident light) one can obtain:

$$r_\sigma \approx 4n_a\cos\phi_a(\eta_1\eta_2)^{-1}\Big\{i\pi(c_{23}\cos\phi_s + P_\sigma n_s c_{13})(d/\lambda)$$

$$+\pi^2\Big[n_s c_{12}c_{23} + P_\sigma c_{13}c_{21}\cos\phi_s + (c_{23}\cos\phi_s + P_\sigma n_s c_{13})(n_s\cos\phi_s - P_\sigma c_{11})$$

$$-2(c_{23}\cos\phi_s + P_\sigma n_s c_{13})\big((c_{43} + n_a n_s\cos\phi_a\cos\phi_s)\eta_1^{-1}$$

$$+(c_{12}n_a n_s + c_{21}\cos\phi_a\cos\phi_s)\,\eta_2^{-1}\big)\Big](d/\lambda)^2\Big\}, \qquad (35)$$

$$\eta_1 \equiv n_a \cos\phi_a + n_s \cos\phi_s, \quad \eta_2 \equiv n_a \cos\phi_s + n_s \cos\phi_a,$$

where $\sigma = ps$ or sp, $P_{ps} = +1$, $P_{sp} = -1$, and

$$
\begin{aligned}
t_\sigma =\ & 2g_\sigma(\eta_1\eta_2)^{-1}n_a\cos\phi_a\big\{i2\pi\gamma_\sigma(d/\lambda) + 2\pi^2\big[K_\sigma\gamma_\sigma + c_{23}(c_{11} + L_\sigma c_{12}) \\
& + c_{13}(c_{21} + L_\sigma c_{11}) - 2\gamma_\sigma(c_{11} + \beta + \alpha)\big](d/\lambda)^2,
\end{aligned}
\tag{36}
$$

where $\gamma_\sigma \equiv c_{23} + L_\sigma c_{13}$, $g_{ps} = \cos\phi_s$, $g_{sp} = \cos\phi_a$, $K_{ps} = n_a\cos\phi_a$, $K_{sp} = n_s\cos\phi_s$, $L_{ps} = n_s/\cos\phi_s$, $L_{sp} = n_a/\cos\phi_a$.

The reflectances $R_{ss} = |r_{ss}|^2$, $R_{pp} = |r_{pp}|^2$, $R_{sp} = |r_{sp}|^2$, and $R_{ps} = |r_{ps}|^2$ are equal to zero in the first order in d/λ. The second-order formulas take the form:

$$
\begin{aligned}
R_{ss} \approx\ & R_s^{(0)}\Big\{1 + 16\pi^2 n_a n_s \cos\phi_a \cos\phi_s(\varepsilon_a - \varepsilon_s)^{-1} \\
& \times\Big[\big(c_{43} - \varepsilon_s\cos^2\phi_s\big)\big(c_{43} - \varepsilon_a\cos^2\phi_a\big)(\varepsilon_a - \varepsilon_s)^{-1} - \big(c_{13}^2 n_a n_s \\
& + c_{23}^2\cos\phi_a\cos\phi_s\big)\big(n_a n_s\cos^2\phi_s + \varepsilon_s\cos\phi_a\cos\phi_s\big)^{-1}\Big](d/\lambda)^2\Big\},
\end{aligned}
\tag{37}
$$

$$
\begin{aligned}
R_{pp} \approx\ & R_p^{(0)}\Big\{1 + 16\pi^2 n_a n_s\cos\phi_a\cos\phi_s\big(\varepsilon_a\cos^2\phi_s - \varepsilon_s\cos^2\phi_a\big)^{-1} \\
& \Big[\big(c_{21}\cos^2\phi_s - c_{12}\varepsilon_s\big) \times \big(c_{21}\cos^2\phi_a - c_{12}\varepsilon_a\big)\big(\varepsilon_a\cos^2\phi_s - \varepsilon_s\cos^2\phi_a\big)^{-1} \\
& + \big(c_{13}^2\varepsilon_s - c_{23}^2\cos^2\phi_s\big)\times(n_a n_s\cos\phi_a\cos\phi_s + \varepsilon_s\cos^2\phi_s)^{-1}\Big](d/\lambda)^2\Big\},
\end{aligned}
\tag{38}
$$

$$
R_\sigma = 16\pi^2\varepsilon_a\cos^2\phi_a(\eta_1\eta_2)^{-2}\left[(c_{23}\cos\phi_s + P_\sigma c_{13}n_s)(d/\lambda)\right]^2,
\tag{39}
$$

where $R_s^{(0)} = |r_s^{(0)}|^2$ and $R_p^{(0)} = |r_p^{(0)}|^2$.

The transmittances

$$
\begin{aligned}
T_{ss} =\ & T_s^{(0)}\big\{1 - 4\pi^2\big[2(c_{13}n_a + c_{23}\cos\phi_a)(c_{13}n_s + c_{23}\cos\phi_s)(\eta_1\eta_2)^{-1} \\
& - 2c_{13}c_{23}(n_a\cos\phi_a + n_s\cos\phi_s)^{-1} - c_{43} + \beta^2\big](d/\lambda)^2\big\},
\end{aligned}
\tag{40}
$$

$$
\begin{aligned}
T_{pp} =\ & T_p^{(0)}\big\{1 - 4\pi^2\big[2(c_{13}n_s + c_{23}\cos\phi_s)(c_{13}n_a + c_{23}\cos\phi_a)(\eta_1\eta_2)^{-1} \\
& - c_{12}c_{21} + \alpha^2\big](d/\lambda)^2\big\},
\end{aligned}
\tag{41}
$$

where

$$T_s^{(0)} = 4n_a n_s\cos\phi_a\cos\phi_s(n_a\cos\phi_a + n_s\cos\phi_s)^{-2}, \tag{42}$$

$$T_p^{(0)} = 4n_a n_s\cos\phi_a\cos\phi_s(n_a\cos\phi_s + n_s\cos\phi_a)^{-2}, \tag{43}$$

are the transmittances for the substrate. The remaining two transmittances T_{sp} and T_{ps} can be calculated from the relation

$$T_\sigma = n_s\cos\phi_s(n_a\cos\phi_a)^{-1}\left|t_\sigma\right|^2. \tag{44}$$

4. ACCURACY OF APPROXIMATE EXPRESSIONS

In this section, approximate analytical results obtained above are correlated with the exact computer solution of the reflection problem for a multilayer system of anisotropic homogeneous films. The main question is, what is the accuracy of approximate formulas. For exact analysis of reflection characteristics we find the four periodic solutions of Eq. (19):

$$\Xi_j(z) = e^{i\frac{2\pi}{\lambda}q_j z}\Xi_j(0), \tag{45}$$

where $j = 1, 2, 3, 4$ and the four eigenvalues q_j can be obtained from the quartic polynomial equation in q:

$$q^4 - 2c_{11}q^3 + \left(c_{11}^2 - c_{12}c_{21} - c_{43}\right)q^2 + 2(c_{11}c_{43} - c_{13}c_{23})q$$
$$+2c_{11}c_{13}c_{23} + c_{12}c_{21}c_{43} - c_{11}^2 c_{43} - c_{13}^2 c_{21} - c_{23}^2 c_{12} = 0, \tag{46}$$

which results from expanding the determinant in the secular equation

$$\text{Det}(\mathbf{C} - q\mathbf{I}) = 0, \tag{47}$$

where $\mathbf{I}$ is the 4×4 unit matrix. Next, for the eigenvectors $\Xi_j(0)$ one can find the following expression:

$$\Xi_j(0) = \begin{bmatrix} 1 \\ a_j/d_j \\ b_j/d_j \\ q_j b_j/d_j \end{bmatrix}, \tag{48}$$

in which

$$a_j \equiv c_{23}(q_j - c_{11}) + c_{13}c_{21}, \tag{49}$$
$$b_j \equiv (q_j - c_{11})^2 - c_{12}c_{21}, \tag{50}$$
$$d_j \equiv c_{13}(q_j - c_{11}) + c_{12}c_{23}, \tag{51}$$

and the exact partial transfer matrix $\mathbf{B}_{ex}$ can be calculated from the relation

$$\mathbf{B}_{ex}(d) = \mathbf{G}\ \Gamma[\mathbf{G}]^{-1}, \tag{52}$$

where 4×4 matrix

$$\mathbf{G} = [\Xi_1(0)\ \Xi_2(0)\ \Xi_3(0)\ \Xi_4(0)], \tag{53}$$

and $\Gamma \equiv \|\gamma_{km}\|$ is a diagonal 4×4 matrix with elements $\gamma_{kk} = \exp(i2\pi q_k d/\lambda)$ and $\gamma_{km} = 0$ if $k \neq m$. Finally, the exact reflection and transmission coefficients can be obtained from the relation (26), where instead of $\mathbf{B}_{ap}^{-1}$ must be used the accurate transfer matrix $\mathbf{B}^{-1}$. Note that to eliminate errors in the computer calculations, we utilized also another, different algorithm, where the eigenvalue problem (47) was directly numerically solved on a computer.

The results of computer simulations for reflection characteristics are plotted in Figs. 2–4. Since in the case of ultrathin films the experimental error of the overall reflectance $R_{pp,ss}$, as a rule, is greater than the contribution of an ultrathin film to $R_{pp,ss}$ then in the subsequent discussion our interest is in differential quantities, e.g., in the relative change of reflectance $\Delta R_{pp,ss}/R_{p,s}^{(0)} \equiv (R_{pp,ss} - R_{p,s}^{(0)})/R_{p,s}^{(0)}$, which is directly brought on by an ultrathin layer. The reason is that the differential reflectance $\Delta R_{pp,ss}/R_{p,s}^{(0)}$ is an immediately measurable quantity because the relative change in the intensity of the reflected
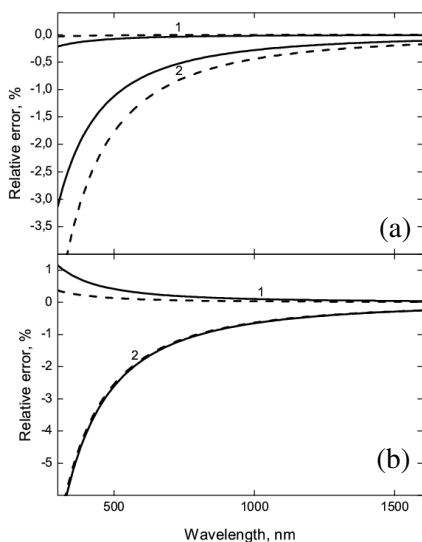
Figure 2. Relative errors of approximate formulas for (a) $\Delta R_{pp}/R_p^{(0)}$ (solid curves), $\Delta R_{ss}/R_s^{(0)}$ (dashed curves) and for (b) R_{ps} (solid curves), R_{sp} (dashed curves) as functions of λ for anisotropic ultrathin films with $d = 3\,\text{nm}$, $n_{xx} = 1.6$ (1), 3.5 (2), $n_{yy} = 1.8$ (1), 3.2 (2), $n_{zz} = 1.5$ (1), 3.8 (2), $\theta = 60°$, $\varphi = 50°$, $\psi = 20°$ at $n_s = 2.5$ and $\phi_a = 45°$. Preceding numbers in parentheses are curve labels.
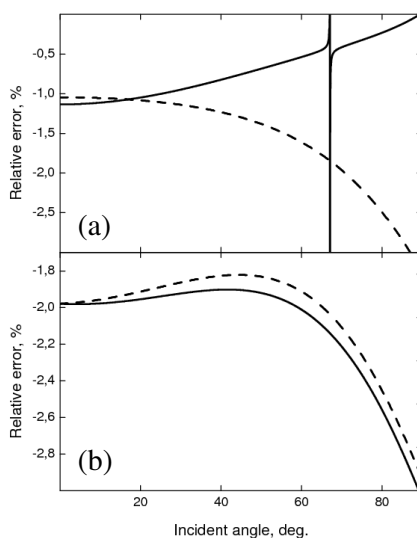
Figure 3. Relative errors of approximate formulas for (a) $\Delta R_{pp}/R_p^{(0)}$ (solid curve), $\Delta R_{ss}/R_s^{(0)}$ (dashed curve) and for (b) R_{ps} (solid curve), R_{sp} (dashed curve) as functions of incident angle ϕ_a for an anisotropic ultrathin film with $d = 5\,\text{nm}$, $n_{xx} = 2.5$, $n_{yy} = 2.4$, $n_{zz} = 2.3$, $\theta = 80°$, $\varphi = 30°$, $\psi = 60°$ at $n_s = 1.5$ and $\lambda = 630\,\text{nm}$.
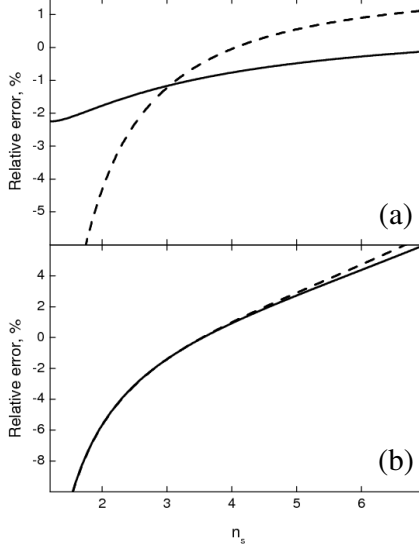
Figure 4. Relative errors of approximate formulas for (a) $\Delta R_{pp}/R_p^{(0)}$ (solid curve), $\Delta R_{ss}/R_s^{(0)}$ (dashed curve) and for (b) R_{ps} (solid curve), R_{sp} (dashed curve) as functions of n_s for an anisotropic ultrathin film with $d = 6\,\mathrm{nm}$, $n_{xx} = 3.1$, $n_{yy} = 3.15$, $n_{zz} = 3.1$, $\theta = 10°$, $\varphi = \psi = 45°$ at $\phi_a = 60°$ and $\lambda = 630\,\mathrm{nm}$.

signal

$$\Delta I_{pp,ss}/I_{p,s} = (I_{pp,ss} - I_{p,s})/I_{p,s} = \left(R_{pp,ss}I_{p,s}^{(in)} - R_{p,s}^{(0)}I_{p,s}^{(in)} \right)/R_{p,s}^{(0)}I_{p,s}^{(in)}$$

$$\equiv \Delta R_{pp,ss}/R_{p,s}^{(0)}, \tag{54}$$

where $I_{p,s}$ and $I_{pp,ss}$ are the reflected intensities from the bare substrate ($d = 0$) and from the system of ultrathin films on the same substrate, respectively, and $I_{p,s}^{(in)}$ is the intensity of the incident light. In addition, the error of approximate expressions for $R_{pp,ss}$ does not adequately depict the situation because the contribution of an ultrathin layer to the reflectance is extremely small (the substrate is of first importance in the causation of reflectance) and as a result the computational exactness of $R_{pp,ss}$ is, in fact, several orders higher than the corresponding exactness for $\Delta R_{pp,ss}/R_{p,s}^{(0)}$. The relative errors $[(R_\sigma)_{ex} - R_\sigma]/(R_\sigma)_{ex}$ and $[(\Delta R_{ss,pp}/R_{s,p}^{(0)})_{ex} - \Delta R_{ss,pp}/R_{s,p}^{(0)}]/(\Delta R_{ss,pp}/R_{s,p}^{(0)})_{ex}$, where $(R_\sigma)_{ex}$ and $(\Delta R_{ss,pp}/R_{s,p}^{(0)})_{ex}$ were obtained by using the rigorous numerical analysis, and $\Delta R_{ss,pp}/R_{s,p}^{(0)}$, R_σ were calculated by

approximate Equations (37), (38), and (39), respectively (R_σ may also be considered as a differential quantity because $R_\sigma = 0$ if $d = 0$), for two different anisotropic ultrathin films as functions of λ are presented in Fig. 2. Note that the quantities λ and d may be in arbitrary common units (only the ratio d/λ matters), and the ambient refractive index $n_a = 1$ in all the figures. As illustrated, the error of approximate equations does not exceed a few percent if the maximum values of d/λ comprises a few hundredths. This is in good agreement with condition $d/\lambda \ll 1/2\pi$ used in the derivation of these formulas. However, the accuracy of approximate equations for given values of d/λ depends on the values of material dielectric constants as well. This can be understood as a consequence of the fact that reflectivity is a measure of optical mismatch between the ambient and the sample. Because of this, it is difficult to indicate explicitly the value of d/λ where the long-wavelength approximation is broken down (the difference between the exact and approximate theory, for example, is greater than 15 percent). Notice that for ultrathin films with nanometric thickness, the developed approximation theory is highly accurate in the far-infrared part of the electromagnetic spectrum ($d/\lambda \le 10^{-3}$).

The dependence of the accuracy of approximate formulas on the angle of incidence ϕ_a is shown in Fig. 3. One can see that in comparison with s-polarization, the differential reflectance of p-polarization as a function of ϕ_a changes its sign passing through the zero value and the approximate formula is inapplicable (Fig. 3(a)) in principle in the neighborhood of the point where $\Delta R_{pp} \to 0$ (even for d/λ as small as wished) because it is insufficient to restrict oneself to terms of the second order in the expansion in d/λ in the vicinity of this point.

Of special interest is the problem of dependence of the accuracy of approximate formulas on the materials refractive indexes and on the strength of anisotropy of thin films or on the difference of refractive indexes between films and a substrate. The direct computations show that generally the accuracy of approximate expressions is lower in the case of strong anisotropy. The exactness of formulas also decreases if the difference in refractive indexes between films and substrate increases (Fig. 4). However, this decrease in accuracy is of little consequence: the desired exactness can easily be achieved by the use of a longer wavelength.

In addition, at large incident angles than the difference between s- and p-polarization is usually clearly defined, the relative error of the approximate formula for R_{ss} may be significantly greater than the analogous error for R_{pp} (Fig. 4). However, for example, if $\phi_a = 80°$, $n_{xx} = 1.5$, $n_{yy} = 1.55$, and $n_{zz} = 1.45$ (the other parameters are the same as in Fig. 4), then the relative errors of $\Delta R_{pp}/R_p^{(0)}$ and $\Delta R_{ss}/R_s^{(0)}$ are

equal to -0.852% and 0.254%, respectively. Therefore, we can not argue that the error for s-polarization is always greater than the error for p-polarization. The result is governed by the particular parameters of films and substrates and, generally, it is not easy to gain an accurate and coherent impression of how the relative errors of approximate formulas depend on material parameters.

Finally, it might be well to point out that the approximate analytical approach works also in the situations of optical degeneracies [17] that arise when light propagates along one of the optic axes in an anisotropic layer. It is well known that in theses instances the conventional numerical methods turn out to be applicable for computation through the presence of mathematical singularities.

5. REFLECTION DIAGNOSTICS

In what follows, we take a look at the potential applicability of approximate expressions obtained above for the reflection diagnostics of anisotropic ultrathin films. First, we show that all unknown components ε_{11}, ε_{22}, ε_{33}, ε_{12}, ε_{13}, and ε_{23} of the dielectric tensor (1) and also the thickness d of an ultrathin anisotropic layer can be determined from the reflection measurements with the expressions derived above. For instance, on the basis of the measurements of $\Delta R_{pp}/R_p^{(0)} \equiv (R_{pp} - R_p^{(0)})/R_p^{(0)}$, R_{ps}, and R_{sp} at the three different incident angles $\phi_a = \phi_a^{(1)}$, $\phi_a = \phi_a^{(2)}$, and $\phi_a = \phi_a^{(3)}$ we can determine the quantities $\varepsilon_{11} - \varepsilon_{13}^2/\varepsilon_{33} \equiv x$, $\varepsilon_{33}^{-1} \equiv y$ from the following system of equations:

$$
\begin{aligned}
a_{21}x^2 + a_{22}y^2 + a_{23}xy + a_{24}x + a_{25}y + a_{26} = 0, \\
a_{31}x^2 + a_{32}y^2 + a_{33}xy + a_{34}x + a_{35}y + a_{36} = 0,
\end{aligned}
\tag{55}
$$

where

$$
a_{i1} = \cos^2 \phi_s^{(i)} \cos^2 \phi_a^{(i)} - P_i \cos^2 \phi_s^{(1)} \cos^2 \phi_a^{(1)},
\tag{56}
$$

$$
a_{i2} = \varepsilon_a^3 \varepsilon_s \left(\sin^4 \phi_a^{(i)} - P_i \sin^4 \phi_a^{(1)} \right),
\tag{57}
$$

$$
\begin{aligned}
a_{i3} = \varepsilon_a \Big[\varepsilon_a \left(\sin^2 \phi_a^{(i)} \cos^2 \phi_s^{(i)} - P_i \sin^2 \phi_a^{(1)} \cos^2 \phi_s^{(1)} \right) \\
+ \varepsilon_s \left(\sin^2 \phi_a^{(i)} \cos^2 \phi_a^{(i)} - P_i \sin^2 \phi_a^{(1)} \cos^2 \phi_a^{(1)} \right) \Big],
\end{aligned}
\tag{58}
$$

$$
a_{i4} = \varepsilon_a \left(P_i \cos^2 \phi_s^{(1)} - \cos^2 \phi_s^{(i)} \right) + \varepsilon_s \left(P_i \cos^2 \phi_a^{(1)} - \cos^2 \phi_a^{(i)} \right),
\tag{59}
$$

$$
a_{i5} = 2\varepsilon_a^2 \varepsilon_s \left(P_i \sin^2 \phi_a^{(1)} - \sin^2 \phi_a^{(i)} \right),
\tag{60}
$$

$$
a_{i6} = \varepsilon_a \varepsilon_s (1 - P_i),
\tag{61}
$$

$$P_i = \frac{\left(\varepsilon_a \cos^2 \phi_s^{(i)} - \varepsilon_s \cos^2 \phi_a^{(i)}\right)^2}{16\pi^2 n_a n_s \cos \phi_a^{(i)} \cos \phi_s^{(i)} P_1} \left[\frac{\Delta R_{pp}^{(i)}}{R_p^{(0)}} + S_i\right], \tag{62}$$

and $i = 2, 3$;

$$P_1 = \frac{\left(\varepsilon_a \cos^2 \phi_s^{(1)} - \varepsilon_s \cos^2 \phi_a^{(1)}\right)^2}{16\pi^2 n_a n_s \cos \phi_a^{(1)} \cos \phi_s^{(1)}} \left[\frac{\Delta R_{pp}^{(1)}}{R_p^{(0)}} + S_1\right], \tag{63}$$

$$S_j = \pm \frac{\left(n_a \cos \phi_a^{(j)} + n_s \cos \phi_s^{(j)}\right)\left(n_a \cos \phi_s^{(j)} + n_s \cos \phi_a^{(j)}\right)}{n_a \cos \phi_a^{(j)} \left(n_a \cos \phi_s^{(j)} - n_s \cos \phi_a^{(j)}\right)}$$

$$\left[R_{ps}\left(\phi_a^{(j)}\right) R_{sp}\left(\phi_a^{(j)}\right)\right]^{1/2}, \tag{64}$$

and $j = 1, 2, 3$.

The system of two nonlinear Equation (55) can be solved with a computer. On the other hand, rather than solve the nonlinear system, the problem can be reduced to a quartic equation for one unknown. This approach has an advantage over the first method because for solving the quartic equations foolproof methods exist. For unknown y, for instance, one can obtain the following quartic equation:

$$Ay^4 + By^3 + Cy^2 + Dy + F = 0, \tag{65}$$

$$A = a_{11}f_1^2 + a_{12}f_4^2 - a_{13}f_1 f_4, \tag{66}$$

$$B = 2(a_{11}f_1 f_2 + a_{12}f_4 f_5) - a_{13}(f_2 f_4 + f_1 f_5) - a_{14}f_1 f_4 + a_{15}f_4^2, \tag{67}$$

$$C = a_{11}(f_2^2 + 2f_1 f_3) + a_{12}f_5^2 - a_{13}(f_3 f_4 + f_2 f_5)$$
$$\quad - a_{14}(f_2 f_4 + f_1 f_5) + 2a_{15}f_4 f_5 + a_{16}f_4^2, \tag{68}$$

$$D = 2a_{11}f_2 f_3 - a_{13}f_3 f_5 - a_{14}(f_3 f_4 + f_2 f_5) + a_{15}f_5^2 + 2a_{16}f_4 f_5, \tag{69}$$

$$F = a_{11}f_3^2 - a_{14}f_3 f_5 + a_{16}f_5^2, \tag{70}$$

$$f_1 = a_{12}a_{21} - a_{11}a_{22}, \quad f_2 = a_{15}a_{21} - a_{11}a_{25}, \quad f_3 = a_{16}a_{21} - a_{11}a_{26},$$
$$f_4 = a_{13}a_{21} - a_{11}a_{23}, \quad f_5 = a_{14}a_{21} - a_{11}a_{24}.$$

If the quantities x and y are known, then the thickness d can be determined from the expression:

$$(d/\lambda)^2 = P_1 \left(x \cos^2 \phi_s^{(1)} - \varepsilon_s + y\varepsilon_a \varepsilon_s \sin^2 \phi_a^{(1)}\right)^{-1}$$
$$\left(x \cos^2 \phi_a^{(1)} - \varepsilon_a + y\varepsilon_a^2 \sin^2 \phi_a^{(1)}\right)^{-1}. \tag{71}$$

Notice that whilst d/λ is always a real positive quantity, then the right-hand side of Equation (71) must also be a real positive number. Such is

indeed the case if the measurement errors of reflection coefficients are within the normal range. However, if in the course of the calculations it emerges that the right-hand side of Equation (71) has not a positive value, then, obviously, the measurement errors of reflection coefficients are unacceptably great and, of course, on the basis of such experimental results one cannot determine the desired parameters. Thus, Equation (71) provides a good separating filter (diplexer) for great random experimental errors.

The quantities $\varepsilon_{12} - \varepsilon_{13}\varepsilon_{23}/\varepsilon_{33}$ and $\varepsilon_{23}/\varepsilon_{33}$ can simply be determined from the measurements of R_{ps} and R_{sp}. On the basis of the Equation (39) one can obtain that

$$\varepsilon_{12} - \frac{\varepsilon_{13}\varepsilon_{23}}{\varepsilon_{33}} = \frac{K_{ps} + K_{sp}}{2\cos\phi_s}, \tag{72}$$

$$\frac{\varepsilon_{23}}{\varepsilon_{33}} = \frac{K_{sp} - K_{ps}}{2n_a n_s \sin\phi_a}, \tag{73}$$

where

$$K_\sigma = \pm R_\sigma^{1/2} \frac{(n_a \cos\phi_a + n_s \cos\phi_s)(n_a \cos\phi_s + n_s \cos\phi_a)}{4\pi n_a \cos\phi_a} \frac{\lambda}{d}. \tag{74}$$

Consider next the determination of the quantity $\varepsilon_{22} - \varepsilon_{23}^2/\varepsilon_{33}$. We can use for this purpose s-polarized light making measurements of $\Delta R_{ss}/R_s^{(0)} \equiv (R_{ss} - R_s^{(0)})/R_s^{(0)}$. The alternative is to use the reflection mode ellipsometric parameters:

$$r_{pp}/r_{ss} \equiv \tan\Psi_{pp}^{(r)} \exp\left(i\Delta_{pp}^{(r)}\right). \tag{75}$$

For the contributions of an ultrathin film to ellipsometric angles $\delta\Psi_{pp}^{(r)} = \Psi_{pp}^{(r)} - \Psi_0^{(r)}$ and $\delta\Delta_{pp}^{(r)} = \Delta_{pp}^{(r)} - \Delta_0^{(r)}$, where $\Psi_0^{(r)}$ and $\Delta_0^{(r)}$ are the ellipsometric angles of a bare substrate (for non-absorbing substrates $\Delta_0^{(r)} \equiv 0$ and $\Psi_0^{(r)}(\phi_B) = 0$), one can obtain the following first-order formulas:

$$\delta\Delta_{pp}^{(r)} = 4\pi n_a \cos\phi_a \, (\varepsilon_a - \varepsilon_s)^{-1} \left[\left(c_{21} \cos^2\phi_s - c_{12}\varepsilon_s\right)\right.$$
$$\left. \times (\cos^2\phi_a - \varepsilon_a\varepsilon_s^{-1} \sin^2\phi_a)^{-1} - c_{43} + \varepsilon_s \cos^2\phi_s\right] (d/\lambda), \tag{76}$$

if $\phi_a \neq \phi_B = \arctan(n_s/n_a)$ (for $\phi_a = \phi_B$, we have $\delta\Delta_{pp}^{(r)} \approx \pi/2$), and

$$\delta\Psi_{pp}^{(r)} = \pi(\varepsilon_a + \varepsilon_s)^{1/2} \left|[c_{21} - c_{12}(\varepsilon_a + \varepsilon_s)](\varepsilon_a - \varepsilon_s)^{-1}\right| (d/\lambda), \tag{77}$$

if $\phi_a = \phi_B$ (for $\phi_a \neq \phi_B$ the quantity $\delta\Psi_{pp}^{(r)} \sim (d/\lambda)^2$).

From Equation (76), we obtain that

$$\varepsilon_{22} - \frac{\varepsilon_{23}^2}{\varepsilon_{33}} = \varepsilon_s + \frac{c_{21}\cos^2\phi_s - c_{12}\varepsilon_s}{\cos^2\phi_a - \varepsilon_a\varepsilon_s^{-1}\sin^2\phi_a} - \delta\Delta_{pp}^{(r)} \frac{(\varepsilon_a - \varepsilon_s)}{4\pi n_a \cos\phi_a} \frac{\lambda}{d}, \tag{78}$$

For determining all components of the dielectric tensor (1) there is a need to evaluate the quantity ε_{13}. All one has to do is to measure the transmission mode ellipsometric parameter $\Delta_{pp}^{(t)}$ because in the case of transmission ellipsometry, where

$$t_{pp}/t_{ss} \equiv \tan \Psi_{pp}^{(t)} \exp\left(i\Delta_{pp}^{(t)}\right), \tag{79}$$

one can obtain that

$$\Delta_{pp}^{(t)} = 2\pi \left[c_{11} + (c_{21}\cos\phi_a\cos\phi_s + n_a n_s c_{12})(n_a\cos\phi_s + n_s\cos\phi_a)^{-1} \right.$$
$$\left. -(n_a n_s \cos\phi_a \cos\phi_s + c_{43})(n_a\cos\phi_a + n_s\cos\phi_s)^{-1}\right](d/\lambda), \tag{80}$$

whence it follows that

$$\frac{\varepsilon_{13}}{\varepsilon_{33}} = \frac{1}{n_a \sin\phi_a}$$
$$\left[\frac{c_{21}\cos\phi_a\cos\phi_s + c_{12}n_a n_s}{n_a\cos\phi_s + n_s\cos\phi_a} - \frac{n_a n_s\cos\phi_a\cos\phi_s + c_{43}}{n_a\cos\phi_a + n_s\cos\phi_s} - \frac{\delta\Delta_{pp}^{(t)}}{2\pi}\frac{\lambda}{d}\right]. \tag{81}$$

Consequently, by the use of reflectance and ellipsometric measurements we can found the quantities ε_{11}, ε_{22}, ε_{33}, ε_{12}, ε_{13}, ε_{23} and then on the basis of the Equations (2)–(7) work out the six desired parameters of anisotropy: ε_{xx}, ε_{yy}, ε_{zz}, θ, φ, and ψ. But the corresponding system of six equations for these unknown quantities is difficult to tackle analytically and, generally, this system can be solved with a computer. Here, we consider solely a couple of cases where one parameter of anisotropy is known, i.e., we have only five unknown quantities. In this situation, the analytical resolution of the issue presents no special problem. For instance, if the angle ψ is known and for simplicity we suppose that $\psi = 0$, then we can obtain the following system of five equations for five unknown quantities ε_{xx}, ε_{yy}, ε_{zz}, θ, φ:

$$\varepsilon_{xx} + \varepsilon_{yy} + \varepsilon_{zz} = \varepsilon_{11} + \varepsilon_{22} + \varepsilon_{33},$$
$$\varepsilon_{yy}\sin^2\theta + \varepsilon_{zz}\cos^2\theta = \varepsilon_{33},$$
$$(\varepsilon_{yy} - \varepsilon_{zz})^2\cos^2\theta\sin^2\theta = \varepsilon_{13}^2 + \varepsilon_{23}^2, \tag{82}$$
$$\varepsilon_{xx}\sin^2\varphi + \left(\varepsilon_{yy}\cos^2\theta + \varepsilon_{zz}\sin^2\theta\right)\cos^2\varphi = \varepsilon_{22},$$
$$(\varepsilon_{zz} - \varepsilon_{yy})\cos\theta\sin\theta\sin\varphi = \varepsilon_{13}$$

The solution of this system has the form:

$$\varepsilon_{xx} = (\varepsilon_{22}\varepsilon_{13}^2 - \varepsilon_{11}\varepsilon_{23}^2)/(\varepsilon_{13}^2 - \varepsilon_{23}^2), \tag{83}$$
$$\varepsilon_{zz} = (\varepsilon_D - \varepsilon_{xx})/2$$
$$\pm \left\{ (\varepsilon_D - \varepsilon_{xx})^2/4 + \varepsilon_{13}^2 + \varepsilon_{23}^2 + \varepsilon_{33}^2 - \varepsilon_{33}(\varepsilon_D - \varepsilon_{xx})\right\}^{1/2}, \tag{84}$$

$$\varepsilon_{yy} = \varepsilon_D - \varepsilon_{xx} - \varepsilon_{zz}, \tag{85}$$

$$\theta = \arcsin[(\varepsilon_{33} - \varepsilon_{zz})/(\varepsilon_{yy} - \varepsilon_{zz})]^{1/2}, \tag{86}$$

$$\varphi = \arcsin[\varepsilon_{13}^2/(\varepsilon_{13}^2 + \varepsilon_{23}^2)]^{1/2}, \tag{87}$$

where $\varepsilon_D = \varepsilon_{11} + \varepsilon_{22} + \varepsilon_{33}$.

Analogously it can be shown that if $\varphi = 0$ then

$$\varepsilon_{xx} = \left\{ \varepsilon_P + \varepsilon_{11} \pm \left[(\varepsilon_P - \varepsilon_{11})^2 + 4\left(\varepsilon_{12}^2 + \varepsilon_{13}^2\right) \right]^{1/2} \right\}/2, \tag{88}$$

$$\varepsilon_{yy} = \varepsilon_{11} + \varepsilon_P - \varepsilon_{xx}, \tag{89}$$

$$\varepsilon_{zz} = \varepsilon_D - \varepsilon_{xx} - \varepsilon_{yy}, \tag{90}$$

$$\theta = \arctan(\varepsilon_{13}/\varepsilon_{12}), \tag{91}$$

$$\psi = \arcsin[(\varepsilon_{xx} - \varepsilon_{11})/(\varepsilon_{xx} - \varepsilon_{yy})]^{1/2}, \tag{92}$$

where $\varepsilon_P = (\varepsilon_{33}\varepsilon_{13}^2 - \varepsilon_{22}\varepsilon_{12}^2)/(\varepsilon_{13}^2 - \varepsilon_{12}^2)$, and if $\theta = 0$ then

$$\varepsilon_{xx} = \left\{ \varepsilon_{11} + \varepsilon_{22} \pm \left[(\varepsilon_{11} - \varepsilon_{22})^2 + 4\varepsilon_{12}^2 \right]^{1/2} \right\}/2, \tag{93}$$

$$\varepsilon_{yy} = \varepsilon_{11} + \varepsilon_{22} - \varepsilon_{xx}, \tag{94}$$

$$\varepsilon_{zz} = \varepsilon_{33} \tag{95}$$

$$\varphi + \psi = \arcsin[(\varepsilon_{22} - \varepsilon_{yy})/(\varepsilon_{xx} - \varepsilon_{yy})]^{1/2}. \tag{96}$$

As may be inferred from the Equation (96) in the later case ($\theta = 0$) we can determine only the sum of two angles φ and ψ.

For reference, we have included a computer simulation for the possible errors of approximate formulas (71), (83)–(87), and (88)–(92) (Figs. 5–9). Computer simulations offer a clearer view of how the approximate formulas work because such approach makes it possible to analyze more complicated situations than we can create in real experiments. It can be said with confidence that expressly this moment is an important benefit to the harnessing of computer simulations. In order to calculate the error of these equations we give certain exact values for all unknown parameters d, ε_{xx}, ε_{yy}, ε_{zz}, θ, φ, ψ and then calculate by the exact electromagnetic theory the values of $\Delta R_{pp}/R_p^{(0)}$, R_σ, $\delta\Delta_{pp}^{(r)}$, and $\Delta_{pp}^{(t)}$. Next, we use these quantities in the form of $\Delta R_{pp}/R_p^{(0)}(1 - v_{pp})$, $R_\sigma(1 - v_\sigma)$, $\delta\Delta_{pp}^{(r)}(1 - v_{\Delta r})$, and $\delta\Delta_{pp}^{(t)}(1 - v_{\Delta t})$ {where v_{pp}, v_σ, $v_{\Delta r}$, and $v_{\Delta t}$ represent the relative errors of $\Delta R_{pp,ss}/R_{p,s}^{(0)}$, R_σ, $\delta\Delta_{pp}^{(r)}$, and $\Delta_{pp}^{(t)}$ respectively} in Equations (62), (63), (64), (74), (78), and (81) for calculating, firstly, the quantities $\varepsilon_{11}^{(calc)}$, $\varepsilon_{22}^{(calc)}$, $\varepsilon_{33}^{(calc)}$, $\varepsilon_{12}^{(calc)}$, $\varepsilon_{13}^{(calc)}$, $\varepsilon_{23}^{(calc)}$, and $d^{(calc)}$ and then for determining $\varepsilon_{xx}^{(calc)}$, $\varepsilon_{yy}^{(calc)}$, $\varepsilon_{yy}^{(calc)}$, $\theta^{(calc)}$, and $\varphi^{(calc)}$ on the basis of

Figure 5. Relative errors of approximate formulas (a) (83) (dash-dotted curve), (84) (solid curve), and (85) (dashed curve) and (b) (86) (dash-dotted curve), (87) (dashed curve), and (71) (solid curve) as functions of λ for an anisotropic ultrathin film with $d = 2\,\mathrm{nm}$, $n_{xx} = 2.4$, $n_{yy} = 2.6$, $n_{zz} = 2.8$, $\theta = 40°$, $\varphi = 60°$, and $\psi = 0$ at $n_s = 1.46$, $\phi_a^{(1)} = 30°$, $\phi_a^{(2)} = 50°$, $\phi_a^{(3)} = 75°$, and $v_{ps} = v_{sp} = v_{\Delta r} = v_{\Delta t} = 0$.
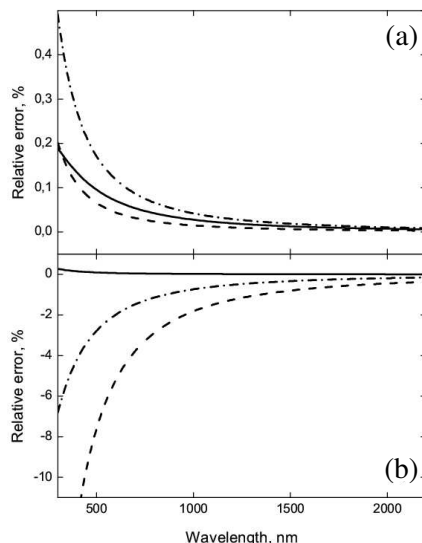
Figure 6. Relative errors of approximate formulas (a) (88) (dash-dotted curve), (89) (dashed curve), and (90) (solid curve) and (b) (91) (dash-dotted curve), (92) (dashed curve), and (71) (solid curve) as functions of λ for an anisotropic ultrathin film with $d = 8\,\mathrm{nm}$, $n_{xx} = 1.46$, $n_{yy} = 1.48$, $n_{zz} = 1.52$, $\theta = 70°$, $\varphi = 0$, and $\psi = 20°$ at $n_s = 2.5$, $\phi_a^{(1)} = 40°$, $\phi_a^{(2)} = 60°$, $\phi_a^{(3)} = 20°$, and $v_{ps} = v_{sp} = v_{\Delta r} = v_{\Delta t} = 0$.

Equations (83)–(87), if $\psi = 0$ or $\varepsilon_{xx}^{(calc)}$, $\varepsilon_{yy}^{(calc)}$, $\varepsilon_{yy}^{(calc)}$, $\theta^{(calc)}$, and $\psi^{(calc)}$ on the basis of Equations (88)–(92), if $\varphi = 0$. The machine performed computations of the relative errors $(\varepsilon_{xx} - \varepsilon_{xx}^{(calc)})/\varepsilon_{xx}$, $(\varepsilon_{yy} - \varepsilon_{yy}^{(calc)})/\varepsilon_{yy}$, $(\varepsilon_{zz} - \varepsilon_{zz}^{(calc)})/\varepsilon_{zz}$, $(\theta - \theta^{(calc)})/\theta$, $(\varphi - \varphi^{(calc)})/\varphi$, and $(\psi - \psi^{(calc)})/\psi$ as functions of λ for $v_{ps} = v_{sp} = v_{\Delta r} = v_{\Delta t} = 0$ are plotted in Figs. 5 and 6. Note that, if $v_{pp} = v_{ss} = v_{ps} = v_{sp} = 0$, then we obtain the pure mathematical error of the approximate formulas that has nothing to do with the error of $\Delta R_{pp,ss}/R_{p,s}^{(0)}$ and R_σ that occurs in the experimental measurements of these quantities. The influence of
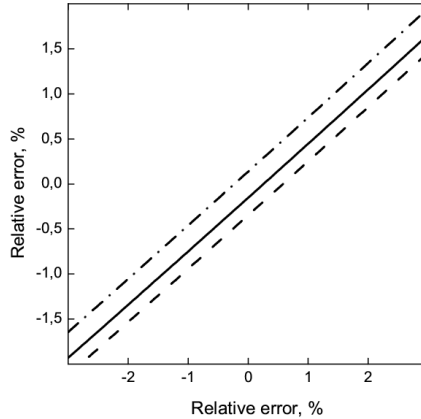
Figure 7. Relative error of the approximate formula (71) versus relative error of $\Delta R_{pp}/R_p^{(0)}$ at $\lambda = 1000\,\text{nm}$, $v_{ps} = v_{sp} = v_{\Delta r} = v_{\Delta t} = 0$ (solid curve), $v_{ps} = v_{sp} = 2\%$ and $v_{\Delta r} = v_{\Delta t} = 1\%$ (dashed curve), and $v_{ps} = v_{sp} = -3\%$ and $v_{\Delta r} = v_{\Delta t} = -2\%$ (dash-dotted curve) for an anisotropic ultrathin film with the same parameters as in Fig. 4.

experimental error of R_σ and $\Delta R_{ss,pp}/R_{s,p}^{(0)}$ is demonstrated in Figs. 7–9. These calculations show that the wavelength plays a role in the error formation only in the short-wavelength region where d/λ is not a sufficiently small quantity. But, in the long-wavelength region the error of approximate formulas is of no concern: the error of desired anisotropic constants is completely defined by instrumental error.

It is necessary to stress that a quartic equation gives generally four different solution, then it may be that Equation (65) yields several real positive solutions for ε_{33}. However, computer simulations show that frequently only one solution of Equation (65) is physically meaningful, i.e., is greater than unity. On the other hand, if two (or even more) real solutions of Equation (65) are > 1, then, of course, one needs to find all final solutions for ε_{xx}, ε_{yy}, ε_{zz}, θ, φ, ψ, and d that follow from different solutions of Equation (65). It is apparent that a mathematical model generates all possible combinations of parameters which possess identical reflection characteristics (the greater the number of parameters, the greater the probability that such different combinations exist). Hence, if two (or more) dissimilar combinations of optical constants and thickness that are all physically meaningful exist among final solutions, then more information (or a combination of optical methods and alternate metrology techniques) is needed for the separation of a true value of the set of optical parameters for the biaxial
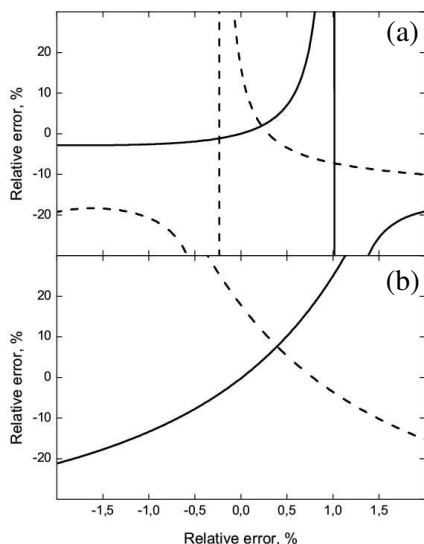
Figure 8. Relative error of approximate formulas (a) (83) and (b) (87) versus relative error of $\Delta R_{pp}/R_p^{(0)}$ at $\lambda = 1500\,\text{nm}$, $v_{ps} = v_{sp} = v_{\Delta r} = v_{\Delta t} = 0$ (solid curves) and $v_{ps} = v_{sp} = -3\%$, $v_{\Delta r} = v_{\Delta t} = -2\%$ (dashed curves) for an anisotropic ultrathin film with the same parameters as in Fig. 4.
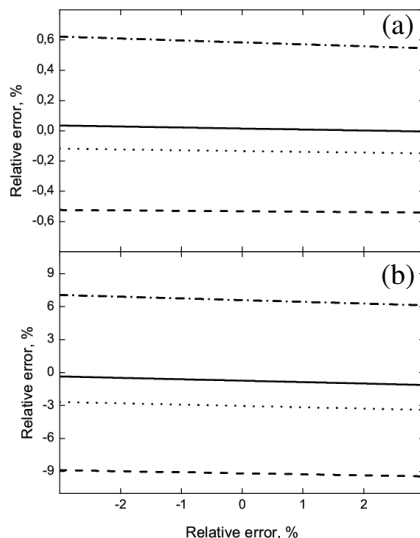
Figure 9. Relative error of approximate formulas (a) (89) and (b) (91) versus relative error of R_σ ($v_{ps} = v_{sp}$) if $\lambda = 1000\,\text{nm}$, $v_{pp} = v_{\Delta r} = v_{\Delta t} = 0$ (solid curves), $v_{pp} = 2\%$, $v_{\Delta r} = v_{\Delta t} = 0$ (dashed curves), $v_{pp} = 0$, $v_{\Delta r} = v_{\Delta t} = 0.5\%$ (dash-dotted curves), and $v_{pp} = -2\%$, $v_{\Delta r} = -1\%$, $v_{\Delta t} = 1\%$ (dotted curves) for an anisotropic ultrathin film with the same parameters as in Fig. 5.

ultrathin film to be investigated. Note that the elucidation of the proper solution in computer simulations should present no problems because, with reduction in d/λ, one can always increase the accuracy of such calculations in a way that one possible solution virtually agrees with given film parameters.

6. CONCLUSION

The analytical approach developed in this paper not only provides insight into the nature of reflection problem for anisotropic films on transparent materials but also furnishes the methods for determining

simultaneously the dielectric constants and thickness of ultrathin anisotropic films. Namely the latter feature of obtained analytical expressions for reflection characteristics is currently of first importance in optics of ultrathin films because the standard regression methods for determining the parameters of ultrathin films on the basis of reflection measurements are characterized by a strong correlation between film thickness and dielectric response. Concurrently performed numerical calculations show that the accuracy of the long-wavelength approximation is reasonable if $d/\lambda \leq a$ few hundredths. Thus, if we use the visible region of wavelengths for measurements, then the thickness of surface layers cannot be in excess of several nanometers. In this case physically in the category of ultrathin films fall, e.g., such layers as native oxides, adsorbed monolayers, Langmuir-Blodgett films, and gate oxides (nanometer-size insulating films) on microelectronic devices. In fact, at the moment of interest are also the possibilities of optical diagnostics for the analysis of utrathin films less than 1 nm thick [8] because expressly this technique is of primary importance in real-time control of deposition and applications involving preparation of next-generation (opto) electronic devices. Generally, in the present context the concept of "ultrathin" should not be taken too literally. For example, in the far infrared region of wavelengths the suggested methods, in principle, can be used in reflection diagnostics of conventional thin films, i.e., the layer thicknesses can even be close to visual wavelengths as well.

REFERENCES

1. Yeh, P., *Optical Waves in Layered Media*, John Wiley & Sons, New York, 2005.

2. Hodgkinson, I. J. and Q. H. Wu, *Birefringent Thin Films and Polarizing Elements*, World Scientific, Singapore, 1997.

3. Robertson, J., "High dielectric constant gate oxides for metal oxide Si transistors," *Rep. Prog. Phys.*, Vol. 69, 327–396, 2006.

4. Zhang, H., R. Solanki, B. Roberds, G. Bai, and I. Banerjee, "High permittivity thin film nanolaminates," *J. Appl. Phys.*, Vol. 87, 1921–1924, 2000.

5. Adamson, P., "Reflection of light in a long-wavelength approximation from an N-layer system of inhomogeneous dielectric films and optical diagnostics of ultrathin layers. I. Absorbing substrate," *J. Opt. Soc. Am. B*, Vol. 20, 752–759, 2003.

6. Adamson, P., "Reflection of light in a long-wavelength approximation from an N-layer system of inhomogeneous dielectric films and

optical diagnostics of ultrathin layers. II. Transparent substrate," *J. Opt. Soc. Am. B*, Vol. 21, 645–654, 2004.

7. Landry, J. P., J. Gray, M. K. O'Toole, and X. D. Zhu, "Incidence-angle dependence of optical reflectivity difference from an ultrathin film on solid surface," *Opt. Lett.*, Vol. 31, 531–533, 2006.

8. Kim, I. K. and D. E. Aspnes, "Analytic determination of n, κ, and d of an absorbing film from polarimetric data in the thin-film limit," *J. Appl. Phys.*, Vol. 101, 033109, 2007.

9. Lekner, J., *Theory of Reflection of Electromagnetic and Particle Waves,* Dordrecht, Martinus Nijhoff, 1987.

10. Hingerl, K., D. E. Aspnes, and I. Kamiya, "Comparison of reflectance difference spectroscopy and surface photoabsorption used for the investigation of anisotropic surfaces," *Surf. Sci.*, Vol. 287/288, 686–692, 1993.

11. Adamson, P., "Reflection of electromagnetic plane waves in a long-wavelength approximation from a multilayer system of anisotropic transparent films on absorbing medium," *Waves in Random and Complex Media*, Vol. 18, 651–668, 2008.

12. Adamson, P., "Laser probing of anisotropic ultrathin dielectric films on absorbing materials via differential reflection characteristics," *Opt. Laser Technol.*, Vol. 41, 424–430, 2009.

13. Adamson, P., "Reflection of electromagnetic plane waves in a long-wavelength approximation from a multilayer system of anisotropic transparent films on non-absorbing medium," *Waves in Random and Complex Media*, Vol. 20, 443–471, 2010.

14. Adamson, P., "Optical diagnostics of anisotropic nanoscale films on transparent isotropic materials by integrating reflectivity and ellipsometry," *Appl. Opt.*, Vol. 48, 5906–5916, 2009.

15. Goldstein, H., *Classical Mechanics,* Addison-Wesley, Reading, 1965.

16. Azzam, R. M. A. and N. M. Bashara, *Ellipsometry and Polarized Light,* Amsterdam, North-Holland, 1977.

17. Xu, W., L. T. Wood, and T. D. Golding, "Optical degeneracies in anisotropic layered media: Treatment of singularities in a 4×4 matrix formalism," *Phys. Rev. B*, Vol. 61, 1740–1743, 2000.